Published in final edited form as:
Mol Cancer Res. 2022 August 05; 20(8): 1295–1304. doi:10.1158/1541-7786.MCR-21-0927.

Exploiting dependence of castration-resistant prostate cancer on the arginine vasopressin signaling axis by repurposing vaptans

Laine M. Heidman,
Nahuel Peinetti,
Valeria A. Copello,
Kerry L. Burnstein
Department of Molecular and Cellular Pharmacology, University of Miami Miller School of Medicine; Sylvester Comprehensive Cancer Center

Abstract

Men with advanced prostate cancer (PC) are treated by androgen deprivation therapy but the disease recurs as incurable castration-resistant prostate cancer (CRPC), requiring new treatment options. We previously demonstrated that the G protein-coupled receptor (GPCR) arginine vasopressin receptor type1A (AVPR1A) is expressed in CRPC and promotes castration resistant growth in vitro and in vivo. AVPR1A is part of a family of GPCR's including arginine vasopressin receptor type 2 (AVPR2). Interrogation of PC patient sample data revealed that co-expression of AVPR1A and AVPR2 is highly correlated with disease progression. Stimulation of AVPR2 with a selective agonist desmopressin promoted CRPC cell proliferation through cAMP/protein kinase A signaling, consistent with AVPR2 coupling to the G alpha s subunit. By contrast, blocking AVPR2 with a selective FDA-approved antagonist, Tolvaptan, reduced cell growth. In CRPC xenografts, antagonizing AVPR2, AVPR1A or both significantly reduced CRPC tumor growth as well as decreased on-target markers of tumor burden. Combinatorial use of AVPR1A and AVPR2 antagonists promoted apoptosis synergistically in CRPC cells. Furthermore, we found that castration-resistant cells produced AVP, the endogenous ligand for arginine vasopressin receptors, and knock-out of *AVP* in CRPC cells significantly reduced proliferation suggesting possible AVP autocrine signaling. These data indicate that the AVP/arginine vasopressin receptor signaling axis represents a promising and clinically actionable target for CRPC.

Corresponding Author: Kerry L. Burnstein, 1600 NW 10th Ave., Rm. 6155 (R189), Miami, FL 33136, Phone: 305-243-3299, kburnstein@med.miami.edu.

AUTHOR CONTRIBUTIONS

L.H. was responsible for experimental design, conducting the research, data analysis and writing. N.P. and V.C. conducted research, analyzed data and assisted with writing. K.L.B. was responsible for experimental design, data analysis, providing funding, and writing.

COMPETING INTERESTS

K.L.B is an inventor on patent US 20160022635A1 submitted by University of Miami that covers "Use of arginine vasopressin receptor antagonists for the treatment of prostate cancer". All other authors declare that they have no competing interests.

INTRODUCTION

Androgen deprivation therapy remains the gold standard for treatment of high risk or advanced prostate cancer (PC) but unfortunately the disease typically recurs as castration-resistant prostate cancer (CRPC). CRPC is currently incurable and thus new therapeutic approaches that exploit actionable targets are needed (1). Aberrant production of arginine vasopressin (AVP, also known as antidiuretic hormone) results in syndrome of inappropriate secretion of antidiuretic hormone (SIADH) and has been observed in some individuals with PC (2–5). Although rare, the presence of SIADH in PC patients is associated with a poorer prognosis (5). AVP is a component of a larger precursor protein (pre-provasopressin), which is cleaved to produce the mature nonapeptide AVP and two other peptides, neurophysin 2 and copeptin. While AVP production occurs primarily in the hypothalamus and is released into circulation from the posterior pituitary in response to increased plasma osmolality, AVP production has also been reported in some breast and small cell lung cancer cell lines where it activates pro-proliferative signaling cascades (6–10).

AVP is the endogenous ligand for a small subfamily of G protein-coupled receptors (GPCRs) which includes arginine vasopressin receptor (AVPR) type 1A, AVPR1B and AVPR2. Our lab previously demonstrated that type 1A (AVPR1A) is expressed in CRPC cells and drives CRPC growth in vitro and in vivo (11). AVP initiates distinct signaling cascades through binding to the different AVP receptors. AVPR1A and AVPR1B couple to the heterotrimeric G protein, G alpha subunit Gq/11, which promotes phospholipase C activity and intracellular calcium release; whereas, AVPR2 signals via the Gs subunit to activate adenylyl cyclase leading to increased intracellular cAMP levels. AVPR1B expression is primarily restricted to the brain, while AVPR1A and AVPR2 are expressed in multiple tissue types. In the kidney, AVPR2 and AVPR1A regulate sodium secretion and water homeostasis (12–13). Co-expression of AVPR1A and AVPR2 alters internalization kinetics of both receptors (14–16) which may influence AVP responsiveness in tissues that contain both receptors.

Analysis of human PC datasets revealed that AVPR1A and AVPR2 expression was significantly co-associated particularly in advanced PC. Since AVPR1A and AVPR2 are expressed in CRPC (11,17,18) and co-expressed in patient tumors, as evidenced by analysis of patient datasets, we examined to what extent AVPR2 contributes to CRPC growth and the effectiveness of dual antagonism of AVPR1A and AVPR2. We found that AVPR2 selective agonism stimulated proliferation and conversely, inhibiting AVPR2 with the FDA-approved AVPR2 antagonist Tolvaptan or by genetic knockdown significantly decreased in vitro PC cell proliferation. Inhibition of AVPR1A and AVPR2, individually or together, with selective antagonists reduced tumor size in vivo as well as markers of tumor growth while having no obvious effect on mouse health, suggesting that the co-expression of AVPR1A and AVPR2 in tumors is a targetable therapeutic vulnerability. Combined suboptimal doses of AVPR1A and AVPR2 antagonists synergistically decreased CRPC cell growth and promoted cell death in vitro with no effect on non-tumorigenic prostate epithelial cells. Furthermore, we demonstrated that CRPC cells were capable of producing AVP and require AVP production for rapid proliferation, consistent with autocrine signaling via AVPR1A and AVPR2 and the existence of a therapeutic window for AVPR antagonism in PC.

MATERIALS & METHODS

Cell culture and reagents

The cell lines RWPE-1, LNCaP, 22Rv1, PC3, and VCaP were obtained from American Type Culture Collection (Manassas, VA). LNCaP, 22Rv1 and PC3 were routinely cultured in RPMI-1640 (Corning Inc., Corning, NY), supplemented with 1% penicillin/streptomycin, 1% l-glutamine (Corning Inc.), and 10% fetal bovine serum (FBS, R&D Systems, Minneapolis, MN) unless otherwise noted. RWPE-1 were cultured in Keratinocyte serum-free media (Corning Inc.) containing recombinant epidermal growth factor and bovine pituitary extract as well as 1% penicillin/streptomycin. VCaP were cultured in DMEM + GlutaMAX (Corning Inc.) containing 10% FBS and 1% anti-mycotic antibiotic (Corning Inc.). The C4-2B cell line was a gift from Dr. Conor Lynch (Moffitt Cancer Center, Tampa, FL), and was cultured in DMEM (Corning Inc.), under the same conditions as LNCaP and 22Rv1. All cell lines were authenticated by STR profiling (Labcorp, Burlington, NC) and routinely tested for mycoplasma (LookOut Mycoplasma PCR Detection Kit, Sigma Aldrich, St. Louis, MO). Cell lines were passaged fewer than 10 times. Trypsin was purchased from Corning Inc. IBMX, Tolvaptan, forskolin, desmopressin (dAVP) and H89 were purchased from Tocris (Bristol, UK). Phenytoin was purchased from Sigma Aldrich. Relcovaptan was purchased from Axon Medchem (Reston, VA).

Bioinformatic analysis of AVP, AVPR1A and AVPR2 expression

The Cancer Genome Atlas Prostate Adenocarcinoma (TCGA-PRAD), GSE70770, and GSE21032 datasets were analyzed for AVPR1A and AVPR2 co-expression via the Xena platform and cBioportal (19–24). AVP expression in microarray data sets GSE6752 (25), GSE89194 (26), GSE35988 (27) and GSE62872 (28), were analyzed in the NCBI GEO database (https://www.ncbi.nlm.nih.gov/geo) (29–30).

RNA analysis

Total RNA was extracted from cells with TRIzol (Invitrogen, Waltham, MA) and the Zymo Direct-zol RNA kit (Zymo Research, Irvine, CA), according to the manufacturer's instructions. cDNA was obtained by reverse-transcribing 1 ug of total RNA using a High-Capacity Reverse Transcription kit (Thermo Fisher, Waltham, MA). Human hypothalamic samples were obtained from the University of Miami Brain Endowment Bank and processed using the RNeasy Lipid Tissue Mini Kit (Qiagen, Hilden, Germany) following manufacturer's instructions.

To determine AVP mRNA expression three-step PCR was done using Go-Taq Green Master Mix (Promega, Madison, WI) for 40 cycles with a melting temperature of 60.5°C for AVP primers and 60°C for HSP90AB1. PCR products were electrophoresed through 4.5% agarose gels with ethidium bromide and bands were observed using Biorad Gel Doc XR System. The following primers were used:

AVP forward – TCCGACCTGGAGCTGAGAC

AVP reverse - GCGACGGCAGGTAGTTCTC

HSP90AB forward – GGGTATCGGAAAGCAAGCCT

HSP90AB reverse – ATGAGGGACATGAGTTGGGC

To determine AVPR2 mRNA expression 100 ng of cDNA was used in RT-qPCR using the QuantStudio3 (Thermo Fisher). Taqman probes (Thermo Fisher) for AVPR2 and GAPDH were used. The relative expression of AVPR2 mRNA was determined by the comparative threshold cycle method. Samples with cycle numbers at least 3 above the No-RT control were considered to be above background.

cAMP ELISA

Cells were incubated overnight in serum free media and the following day treated with 50 μM IBMX for 20 minutes before addition of 1 nM dAVP for 10 or 30 minutes. Cells were harvested and analyzed according to the manufacturer's instructions (Cayman Chemicals, Ann Arbor, MI).

Intracellular calcium release

22Rv1 cells were cultured, treated with different concentrations of dAVP and analyzed for intracellular calcium release as described previously (11).

In vitro cell proliferation

Cells were cultured in media containing 2% FBS or 5% charcoal stripped serum (CSS, Hyclone Laboratories Inc.) as indicated in the figure legends. Unless otherwise stated, after 6 days of growth, cells were trypsinized and stained with trypan blue (Sigma Aldrich) for live versus dead cell counting using the Countess II (Thermo Fisher).

Plasmids and genetic knockdown/overexpression

Plko.1 shGFP was provided by Dr. Priyamvada Rai (University of Miami) and plko.1 shAVPR2 was purchased from Sigma Aldrich. pQCXIN empty vector (EV) was purchased from Clontech. Transduction of cells for shRNA-mediated knockdown of AVPR2 or overexpression of AVPR1A was performed as described previously (11).

Immunoblotting

Protein lysates were prepared and immunoblotted as previously described (11). Hsp90 (610419) antibody was purchased from BD Biosciences (Franklin Lakes, NJ) and used at 1:3000. Cyclin A (sc-751) antibody was purchased from Santa-Cruz Biotechnology Inc. (Dallas, TX) and used at 1:2000. PCNA (13110) antibody (Cell Signaling Technology Danvers, MA) was used at 1:1000 in 5% BSA.

Drug synergism analysis

C4-2B and 22Rv1 cells were cultured in media containing 2% FBS with different concentrations of Relcovaptan and Tolvaptan and were counted 6 days later. The combination index (CI) of Relcovaptan and Tolvaptan was calculated using the software developed by Ting Chao-Chou and Nick Martin, Compusyn. Compusyn is based on Chou-Talalay's Combination Index Theorem (31). The highest concentrations of Relcovaptan and

Tolvaptan yielding greater effect and lower CI than the other concentrations were selected for further growth experiments in RWPE-1, LNCaP, VCaP, and PC3.

Caspase 3/7 activity assays

22Rv1 cells were cultured in media containing 2% FBS and 10 μM Relcovaptan, 5 μM Tolvaptan, or both, as well as the Incucyte Caspase-3/7 Green Dye for Apoptosis (Sartorius, Göttingen, Germany) according to the manufacturer's instructions. Cells were imaged using the Incucyte Zoom (Sartorius) at 10x magnification with phase and green fluorescent image acquisition every 2 hours for 7 days.

Xenograft Tumor Growth

Animal studies were performed after protocol approval by the Institutional Animal Care and Use Committee (IACUC) at the University of Miami. Animals were treated according to the National Institutes of Health (NIH) Guide for the Care and Use of Laboratory Animals. 1×10^6 C4-2B cells were injected bilaterally into the flanks of 5 to 6-week old nu/nu mice (Envigo, Indianpolis, IN) with Matrigel (BD Biosciences). The following day mice were randomly assigned treatment and started on daily IP injections of vehicle, 50 mg/kg Relcovaptan, 12.3 mg/kg Tolvaptan, both or vehicle. Drugs were dissolved in a vehicle of 1:1:8 DMSO:Tween 80:Saline (Sigma Aldrich). Tumors were measured with calipers three times per week single blind. Mouse weights were measured three times per week. After 40 days of treatment mice were sacrificed. Tumors were removed, weighed, imaged and immediately placed in liquid nitrogen. Tumors that were too small to be weighed were removed from the final analysis. Mouse blood samples were taken via cardiac puncture, centrifuged 10,000xg at 4 °C for 10 minutes, and the plasma collected for PSA analysis by ELISA (Biocheck Inc., San Francisco, CA) according to the manufacturer's instructions. Portions of the tumors were paraffin embedded and histologic analyses were performed by Histowiz Inc. (histowiz.com, Brooklyn, NY). Samples were processed according to their workflow for DAB and hematoxylin staining for CD31 and nuclei respectively. Slide images were uploaded to the Leica Aperio Imagescope (Leica Biosystems, Richmond, IL) software and images were taken of tumor sections to be analyzed for CD31 expression in Fiji (ImageJ) using a semi-quantitative method as previously described (32,33). Sections of tumors were prepared as previously described (11). Tumor lysates were analyzed for PCNA by immunoblotting.

Tumor growth curves were compared using ratio of adjusted areas under the curves (aAUCs) method (34). *p*-values were determined using a permutation test of the ratio of the two aAUCs. For tumor weight, PSA, and CD31 expression; ANOVA was used and adjusted p-values for pairwise comparison between groups from Student t-test were obtained based on Tukey's method. For PCNA expression Student t-test was performed for each treatment versus vehicle. Results with p-values < 0.05 were considered statistically significant. Statistical analyses were performed using statistical software package R (version 4.0.3) or GraphPad Prism (version 6).

Copeptin ELISA

Cells were cultured in serum-free media. For RWPE-1, the media was free of recombinant epidermal growth factor and bovine pituitary extract. After 48 hours, cell media were collected and live cells were counted. Conditioned cell media were applied to a C-18 separation column (Phoenix Pharmaceuticals Inc., Burlingame, CA) followed by concentration in a Savant SpeedVac (Thermo Fisher). The pellets were then resuspended in a copeptin ELISA (Phoenix Pharmaceuticals Inc.) buffer and analyzed according to manufacturer's instructions.

AVP gene knockout by CRISPR-Cas9

LentiCRISPR v2 (Addgene plasmid #52961) was a gift from Dr. Feng Zhang. Gene-specific sgRNAs were designed using the CRISPick platform from Broad Institute and cloned into the LentiCRISPR v2 plasmid using Esp3I restriction enzyme (Thermo Fisher). C4-2B cells were transduced and selected with puromycin (2.5μg/ml).

sgRNA sequence was:

sgAVP – CACCGCGGGCCCAGCATCTGCTGCG

Statistical Analysis

Unless otherwise stated, experiments were performed at least 3 times with multiple replicates. Normality for data was determined by Shapiro-Wilk analysis. Unless otherwise stated, data were analyzed for significant differences using GraphPad Prism (version 6) one way ANOVA or Kruskal-Wallis based on normality of data. $P < 0.05$ was considered significant.

Data Availability

The data generated from this study are available within the article and its supplementary files.

RESULTS

AVPR1A and AVPR2 mRNA are highly correlated in advanced prostate cancer

Analysis of PC RNA-seq and microarray datasets from human samples demonstrated significant, positive associations between AVPR1A with AVPR2 expression in cancer (localized and metastatic) but not in benign tissue (Figure 1A,B). Strong association between AVPR1A and AVPR2 was observed in tumors with high Gleason Score (8–10) but not in tumors with low Gleason score 6 (Figure 1C). AVPR1A and AVPR2 are co-expressed in over 95% of patient PC samples in the datasets shown in figure 1.

AVPR2-mediated cell proliferation is dependent upon cAMP/PKA

We found that AVPR2 mRNA was expressed in several PC cell lines (Figure 2A and Supp Fig 1A). To determine the effects of AVPR2 activation, we treated PC cell lines with an AVPR2 selective agonist, desmopressin (dAVP). dAVP treatment increased levels of intracellular cAMP in AVPR2-expressing PC cell lines, but had no effect on intracellular

cAMP in VCaP, which express AVPR1A (11) but not AVPR2 (Figure 2A,B and Supp Fig 1A). Furthermore in 22Rv1 cells, which express both AVPR1A and AVPR2, dAVP only stimulated cAMP production but did not promote intracellular calcium release, which is a canonical AVPR1A effect (Supp Fig 1B). These results confirm in PC that dAVP specifically stimulated AVPR2, which signals via Gs to activate adenylyl cyclase and promote cAMP production.

dAVP had no effect on the proliferation of non-tumorigenic prostate epithelial cell lines, RWPE-1 and BPH-1, or on an androgen-dependent PC cell line, VCaP, that only expresses AVPR1A (Fig 2C and Supp Fig 2A,B). Notably not only did dAVP stimulate proliferation of the CRPC cell lines but dAVP was sufficient to promote growth of androgen-dependent LNCaP cells in media depleted of androgens (Figure 2D) but not in androgen-replete media (Supp Figure 3). This finding suggests that AVPR2 activation is sufficient for castration-resistant growth of LNCaP cells. To determine whether cAMP signaling was required for dAVP-stimulated cell growth, we examined H89 an inhibitor of PKA, a canonical downstream effector of cAMP (35). In all three AVPR2-expressing PC cell lines, H89 blocked dAVP-mediated cell proliferation (Figure 2D).

Given that AVPR2 agonism promoted PC cell growth, we investigated the possible anti-proliferative properties of Tolvaptan, an FDA-approved AVPR2-selective antagonist used for the treatment of hyponatremia (36). Blocking AVPR2 with Tolvaptan decreased growth of PC cell lines that express AVPR2 mRNA, but had no effect on the non-tumorigenic cell lines RWPE-1 and BPH-1 or on VCaP cells (Figure 3A and Supp Fig 2C). In addition, knockdown of AVPR2 using shRNA reduced PC growth but had no effect on VCaP, which lack AVPR2 (Supp Fig 1, Supp Fig 4).

Tolvaptan also decreased cyclin A levels in AVPR2-expressing PC cell lines, indicating that AVPR2 antagonism inhibited cell cycle progression (Figure 3B). Furthermore, the antiproliferative effects of Tolvaptan were partially rescued by co-treatment with forskolin (Figure 3C), which activates adenylyl cyclase and increases intracellular levels of cAMP. Taken together, these data indicate that AVPR2 promotes PC cell proliferation at least in part through activation of the cAMP/PKA signaling cascade.

Dual antagonism of AVPR1A and AVPR2 blocks tumor growth in vivo

Given that co-expression of AVPR1A and AVPR2 is strongly correlated in advanced disease (Figure 1), we evaluated the effect of AVPR1A and AVPR2 antagonism using Relcovaptan, Tolvaptan, or both drugs together on CRPC C4-2B xenografts. All treatments significantly decreased tumor growth and tumor weight (Figure 4 A,B,D) while having no effect on mouse weights (Figure 4C). As expected from our previous work, Relcovaptan also significantly decreased PSA (Figure 4E), a clinically relevant marker of tumor burden; however, while Tolvaptan inhibition of PSA did not quite reach statistical significance (P=0.051), treatment with Relcovaptan and Tolvaptan significantly reduced PSA. Decreased expression of CD31, a tumor biomarker typically associated with tumor vascularization and growth, was observed in all treatment groups compared to vehicle controls (Figure 4F). While dual antagonism of AVPR1A and AVPR2 by Relcovaptan and Tolvaptan significantly reduced tumor growth, weight, circulating PSA and CD31, there was no significant

difference between treatment groups. However, only dual antagonism of AVPR1A and AVPR2 significantly reduced PCNA levels (Figure 4G and Supp Fig 5), a marker of cell cycle progression and proliferation.

Sub-optimal doses of AVPR1A and AVPR2 antagonists synergistically decrease PC cell proliferation

We evaluated lower concentrations of Relcovaptan and Tolvaptan in 22Rv1 and C4-2B in vitro for synergistic growth inhibition. We used CompuSyn (31) to select concentrations that were below levels required for single agent inhibition of cell proliferation for each cell line (Supp Fig 6). Combined treatment with Relcovaptan and Tolvaptan significantly decreased 22Rv1 and C4-2B cell proliferation (Figure 5A) and increased the percentage of dead cells (Figure 5B) over either treatment alone. This combined dose of Relcovaptan and Tolvaptan did not decrease proliferation of cell lines that expressed solely AVPR1A or AVPR2 or neither (Fig. 5A). Furthermore, we found that treatment with both Relcovaptan and Tolvaptan in 22Rv1 CRPC cells significantly increased caspase 3/7 activity over either treatment alone (Figure 5C, D).

Additionally, ectopic expression of AVPR1A in LNCaP cells that normally express only AVPR2, resulted in synergistic growth inhibition by dual antagonism of AVPR1A and AVPR2 (Supp Fig 7). These findings suggest that combined AVPR1A and AVPR2 antagonism may be a particularly effective therapeutic approach in CRPC given that the majority of cases express both receptors.

AVP is synthesized by CRPC cells

As mentioned previously, AVPR1A and AVPR2 belong to the same family of GPCRs with AVP as the common endogenous ligand. To investigate whether CRPC cells participate in autocrine/paracrine signaling, we analyzed AVP mRNA expression in patient sample datasets representing benign, primary (localized) and advanced PC (metastatic CRPC). mRNA encoding pre-provasopressin (from which AVP is derived) was present at higher levels in metastatic CRPC compared to benign tissue or localized disease (Figure 6 A–B). There was no difference in AVP expression in primary site PC compared to normal tissue (Supp Fig 8), consistent with AVP increasing during disease progression.

We detected AVP mRNA in several human PC cell lines, but not in a non-tumorigenic prostate epithelial cell line RWPE-1 (Figure 6C). Analysis of conditioned media by ELISA revealed that two CRPC cell lines secreted copeptin, which is a component of pre-provasopressin and is used clinically as a surrogate marker for the less stable AVP (37). C4-2B, a bone metastatic CRPC derivative of the androgen dependent LNCaP cell line, produced the most copeptin of the PC cell lines examined (Figure 6D). Furthermore, phenytoin, a voltage gated sodium channel blocker that decreases copeptin production in small cell lung cancer cells (10), significantly reduced copeptin in conditioned media of C4-2B cells (Figure 6E). Phenytoin treatment inhibited C4-2B cell growth, which was rescued by treatment with AVP indicating selectivity of phenytoin inhibition of AVP synthesis (Figure 6F). In addition, knocking out the *AVP* gene by CRISPR-Cas9 in C4-2B reduced copeptin production as well as CRPC cell proliferation under castration conditions

in vitro (Figure 6G–H). These data show that AVP can be produced and secreted by CRPC cells consistent with a possible AVP-driven autocrine/paracrine paradigm.

DISCUSSION

Bioinformatic analysis of PC patient sample datasets revealed that AVPR1A and AVPR2 mRNA are co-expressed particularly in advanced and metastatic CRPC thereby revealing a possible avenue for therapy through targeting both receptors. The current study explores the contributions of the AVP/AVPR signaling axis to PC growth and progression as well as the efficacy of combining antagonists for both AVPR1A and AVPR2 in CRPC models in vitro and in vivo.

The AVPR2 selective agonist desmopressin (dAVP) increased intracellular cAMP and stimulated PC cell proliferation that was dependent upon PKA. Indeed under castrate conditions, dAVP was sufficient to promote androgen-dependent LNCaP cell proliferation and *AVP* knock out in CRPC cells decreased proliferation. Conversely, AVPR2 antagonism with Tolvaptan, an FDA approved drug, inhibited the proliferation of PC cells that express AVPR2 but interestingly had no effect on the proliferation of non-tumorigenic prostate epithelial cells despite expression of AVPR2. These data suggest that PC cells have a unique dependence on AVPR2 activity not shared by non-tumorigenic cells. Treatment of PC cells with forskolin to increase intracellular cAMP levels partially rescued the antiproliferative effects of AVPR2 antagonism. Activation of Gs-cAMP-PKA upregulates negative feedback loops mediated by PKA-dependent phosphodiesterases that break down cAMP (38), allowing for tight temporal control of the signaling cascade. Therefore, the partial (but not full) rescue of PC cell proliferation that we observed with forskolin may be due to insufficient sustained increases in intracellular cAMP levels.

Our findings align with the pro-tumorigenic functions of AVPR2 in clear cell renal carcinoma (RCC), as well as with the finding that Tolvaptan inhibits RCC (39). In addition, a recent study found that Tolvaptan inhibits human small cell lung cancer (SCLC) cell growth in vitro in a low sodium environment meant to mimic SIADH (40).

In contrast to the pro-tumorigenic effects of AVPR2, the AVPR2 selective agonist dAVP has been shown to exert anti-tumor effects in a variety of other cancers (41–44). In terms of PC, dAVP modestly decreased proliferation of the human cell line PC3 (17–18) but the effect of AVPR2 antagonism was not examined. The reason for the disparate effect of dAVP in PC3 cells compared to the effects we observed in an array of CRPC cell lines is unknown. PC3 cells, unlike the vast majority of human PC tumors, do not express AR and thus reflect a small subset of clinical PC.

We demonstrate that antagonism of the AVP/AVPR signaling axis greatly decreased CRPC tumor xenograft growth in vivo. Combining Relcovaptan and Tolvaptan decreased all assessed markers of tumor growth and burden (tumor weight, circulating PSA, CD31, PCNA) without affecting mouse weights or having an obvious effect on mouse behavior. Sub-optimal levels of the AVPR1A antagonist, Relcovaptan and the AVPR2 antagonist, Tolvaptan together synergistically reduced CRPC cell proliferation and induced apoptosis

in vitro. Dual inhibiton of AVPR1A and AVPR2 had no effect on non-tumorigenic cells in vitro. Future work will require optimizing concentrations of each of the AVPR antagonists for maximal tumor inhibition by combination vaptan therapy in pre-clinical models of CRPC.

Bioinformatic analysis of PC patient sample datasets revealed increased expression of AVP, the endogenous ligand for both AVPR1A and AVPR2, in advanced forms of PC compared to primary localized tumors consistent with the possibility that CRPC produces AVP. Interestingly, Brattleboro rats, which are unable to synthesize AVP due to a single base deletion within the *AVP* coding region, exhibit decreased growth of a syngeneic sarcoma model compared to WT rats (45). C4-2B, a castration resistant bone metastatic derivative of androgen dependent LNCaP, expressed AVP mRNA and secreted the highest amounts of the AVP surrogate copeptin of the PC cell lines tested. The skeleton is the most common site for PC metastasis where cancer cells promote bone remodeling leading to the deposition of painful bony osteoblastic lesions (46). The current finding that C4-2B secreted AVP has two critical implications. CRPC secretion of AVP may stimulate cancer cell proliferation in an autocrine manner leading to increased cancer-induced bone remodeling. Since osteoblasts and osteoclasts also express AVPR1A and AVPR2 (47), CRPC-produced AVP may further exacerbate bone remodeling in a paracrine fashion. Thus, dual antagonism of AVP receptors may be particularly beneficial in late-stage bone metastatic CRPC (11, see commentary in ref. 48). Together these findings show that the AVP/AVPR1A/AVPR2 signaling axis represents a promising therapeutic target given the possibility of repurposing and combining existing antagonists to AVPRs that have already been proven safe and effective in human clinical trials.

Supplementary Material

Refer to Web version on PubMed Central for supplementary material.

ACKNOWLEDGEMENTS

We gratefully acknowledge the contributions of the Molecular Therapeutics Shared Resource in the Sylvester Comprehensive Cancer Center as well as the University of Miami Brain Endowment Bank and Dr. David Davis for supplying us with hypothalamic tissue. We thank Dr. Zhipeng Meng for advice on CRISPR-Cas9, Fan Yang for his assistance with several experiments and Dr. Deukwoo Kwon for assistance with statistical analysis. We are grateful to Dr. M. Julia Martinez and other Burnstein lab members for helpful comments on the manuscript.

Funding:

This work was supported by VA Merit Review BX002773 (to K.L.B), Developmental Funds from the Sylvester Comprehensive Cancer Center (to K.L.B.) and NCI Funded Sylvester Comprehensive Cancer Center Support Grant (1P30CA240139) (to N.P.)

REFERENCES

1. Wang YA, Sfakianos J, Tewari AK, Cordon-Cardo C, & Kyprianou N (2020). Molecular tracing of prostate cancer lethality. Oncogene, 39(50), 7225–7238. doi:10.1038/s41388-020-01496-5 [PubMed: 33046797]
2. Garzotto M, & Beer TM (2001). Syndrome of inappropriate antidiuretic hormone secretion: a rare complication of prostate cancer. J Urol, 166(4), 1386. [PubMed: 11547083]

3. Fukasawa M, Sawada N, Shimura H, Ihara T, Kira S, Zakoji H, et al. (2017). Successful Radiotherapy for Advanced Small Cell Carcinoma of the Prostate with Syndrome of Inappropriate Secretion of Antidiuretic Hormone. Urol Case Rep, 13, 147–148. doi:10.1016/j.eucr.2017.04.008 [PubMed: 28567332]
4. Shaaban H, Thomas D, & Guron G (2012). A rare case of metastatic ductal type prostate adenocarcinoma presenting with syndrome of inappropriate secretion of antidiuretic hormone: a case report and review. J Cancer Res Ther, 8(2), 308–310. doi:10.4103/0973-1482.98999 [PubMed: 22842384]
5. Yamazaki T, Suzuki H, Tobe T, Sekita N, Kito H, Ichikawa T, et al. (2001). Prostate adenocarcinoma producing syndrome of inappropriate secretion of antidiuretic hormone. Int J Urol, 8(9), 513–516. doi:10.1046/j.1442-2042.2001.00362.x [PubMed: 11683974]
6. Keegan BP, Akerman BL, Pequeux C, & North WG (2006). Provasopressin expression by breast cancer cells: implications for growth and novel treatment strategies. Breast Cancer Res Treat, 95(3), 265–277. doi:10.1007/s10549-005-9024-8 [PubMed: 16331351]
7. Keegan BP, Memoli VA, Wells WA, & North WG (2010). Detection of Provasopressin in Invasive and Non-invasive (DCIS) Human Breast Cancer Using a Monoclonal Antibody Directed Against the C-terminus (MAG1). Breast Cancer (Auckl), 4, 15–22. [PubMed: 20697529]
8. North WG, Wells W, Fay MJ, Mathew RS, Donnelly EM, & Memoli VA (2003). Immunohistochemical evaluation of vasopressin expression in breast fibrocystic disease and ductal carcinoma in situ (DCIS). Endocr Pathol, 14(3), 257–262. doi:10.1007/s12022-003-0018-y [PubMed: 14586071]
9. Pequeux C, Keegan BP, Hagelstein MT, Geenen V, Legros JJ, & North WG (2004). Oxytocin- and vasopressin-induced growth of human small-cell lung cancer is mediated by the mitogen-activated protein kinase pathway. Endocr Relat Cancer, 11(4), 871–885. doi:10.1677/erc.1.00803 [PubMed: 15613460]
10. Ohta T, Mita M, Hishinuma S, Ishii-Nozawa R, Takahashi K, & Shoji M (2017). Inhibition of Ectopic Arginine Vasopressin Production by Phenytoin in the Small Cell Lung Cancer Cell Line Lu-165. Front Endocrinol (Lausanne), 8, 94. doi:10.3389/fendo.2017.00094 [PubMed: 28503166]
11. Zhao N, Peacock SO, Lo CH, Heidman LM, Rice MA, Fahrenholtz CD, et al. (2019). Arginine vasopressin receptor 1a is a therapeutic target for castration-resistant prostate cancer. Sci Transl Med, 11(498). doi:10.1126/scitranslmed.aaw4636
12. Sparapani S, Millet-Boureima C, Oliver J, Mu K, Hadavi P, Kalostian T, . . . Gamberi C (2021). The Biology of Vasopressin. Biomedicines, 9(1). doi:10.3390/biomedicines9010089
13. Koshimizu TA, Nakamura K, Egashira N, Hiroyama M, Nonoguchi H, & Tanoue A (2012). Vasopressin V1a and V1b receptors: from molecules to physiological systems. Physiol Rev, 92(4), 1813–1864. doi:10.1152/physrev.00035.2011 [PubMed: 23073632]
14. Faklaris O, Cottet M, Falco A, Villier B, Laget M, Zwier JM, et al. (2015). Multicolor time-resolved Forster resonance energy transfer microscopy reveals the impact of GPCR oligomerization on internalization processes. FASEB J, 29(6), 2235–2246. doi:10.1096/fj.14-260059 [PubMed: 25690655]
15. Terrillon S, Barberis C, & Bouvier M (2004). Heterodimerization of V1a and V2 vasopressin receptors determines the interaction with beta-arrestin and their trafficking patterns. Proc Natl Acad Sci U S A, 101(6), 1548–1553. doi:10.1073/pnas.0305322101 [PubMed: 14757828]
16. Terrillon S, Durroux T, Mouillac B, Breit A, Ayoub MA, Taulan M, et al. (2003). Oxytocin and vasopressin V1a and V2 receptors form constitutive homo- and heterodimers during biosynthesis. Mol Endocrinol, 17(4), 677–691. doi:10.1210/me.2002-0222 [PubMed: 12554793]
17. Pifano M, Garona J, Capobianco CS, Gonzalez N, Alonso DF, & Ripoll GV (2017). Peptide Agonists of Vasopressin V2 Receptor Reduce Expression of Neuroendocrine Markers and Tumor Growth in Human Lung and Prostate Tumor Cells. Front Oncol, 7, 11. doi:10.3389/fonc.2017.00011 [PubMed: 28194370]
18. Sasaki H, Klotz LH, Sugar LM, Kiss A, & Venkateswaran V (2015). A combination of desmopressin and docetaxel inhibit cell proliferation and invasion mediated by urokinase-type plasminogen activator (uPA) in human prostate cancer cells. Biochem Biophys Res Commun, 464(3), 848–854. doi:10.1016/j.bbrc.2015.07.050 [PubMed: 26182875]

19. Cancer Genome Atlas Research, N. (2015). The Molecular Taxonomy of Primary Prostate Cancer. Cell, 163(4), 1011–1025. doi:10.1016/j.cell.2015.10.025 [PubMed: 26544944]
20. Ross-Adams H, Lamb AD, Dunning MJ, Halim S, Lindberg J, Massie CM, et al. (2015). Integration of copy number and transcriptomics provides risk stratification in prostate cancer: A discovery and validation cohort study. EBioMedicine, 2(9), 1133–1144. doi:10.1016/j.ebiom.2015.07.017 [PubMed: 26501111]
21. Whitington T, Gao P, Song W, Ross-Adams H, Lamb AD, Yang Y, et al. (2016). Gene regulatory mechanisms underpinning prostate cancer susceptibility. Nat Genet, 48(4), 387–397. doi:10.1038/ng.3523 [PubMed: 26950096]
22. Goldman MJ, Craft B, Hastie M, Repecka K, McDade F, Kamath A, et al. (2020). Visualizing and interpreting cancer genomics data via the Xena platform. Nat Biotechnol, 38(6), 675–678. doi:10.1038/s41587-020-0546-8 [PubMed: 32444850]
23. Cerami E, Gao J, Dogrusoz U, Gross BE, Sumer SO, Aksoy BA, et al. (2012). The cBio cancer genomics portal: an open platform for exploring multidimensional cancer genomics data. Cancer Discov, 2(5), 401–404. doi:10.1158/2159-8290.CD-12-0095 [PubMed: 22588877]
24. Gao J, Aksoy BA, Dogrusoz U, Dresdner G, Gross B, Sumer SO, et al. (2013). Integrative analysis of complex cancer genomics and clinical profiles using the cBioPortal. Sci Signal, 6(269), pl1. doi:10.1126/scisignal.2004088 [PubMed: 23550210]
25. Chandran UR, Ma C, Dhir R, Bisceglia M, Lyons-Weiler M, Liang W, et al. (2007). Gene expression profiles of prostate cancer reveal involvement of multiple molecular pathways in the metastatic process. BMC Cancer, 7, 64. doi:10.1186/1471-2407-7-64 [PubMed: 17430594]
26. Ding Y, Wu H, Warden C, Steele L, Liu X, Iterson MV, et al. (2016). Gene Expression Differences in Prostate Cancers between Young and Old Men. PLoS Genet, 12(12), e1006477. doi:10.1371/journal.pgen.1006477 [PubMed: 28027300]
27. Grasso CS, Wu YM, Robinson DR, Cao X, Dhanasekaran SM, Khan AP, et al. (2012). The mutational landscape of lethal castration-resistant prostate cancer. Nature, 487(7406), 239–243. doi:10.1038/nature11125 [PubMed: 22722839]
28. Penney KL, Sinnott JA, Tyekucheva S, Gerke T, Shui IM, Kraft P, et al. (2015). Association of prostate cancer risk variants with gene expression in normal and tumor tissue. Cancer Epidemiol Biomarkers Prev, 24(1), 255–260. doi:10.1158/1055-9965.EPI-14-0694-T [PubMed: 25371445]
29. Barrett T, Wilhite SE, Ledoux P, Evangelista C, Kim IF, Tomashevsky M, et al. (2013). NCBI GEO: archive for functional genomics data sets--update. Nucleic Acids Res, 41(Database issue), D991–995. doi:10.1093/nar/gks1193 [PubMed: 23193258]
30. Edgar R, Domrachev M, & Lash AE (2002). Gene Expression Omnibus: NCBI gene expression and hybridization array data repository. Nucleic Acids Res, 30(1), 207–210. doi:10.1093/nar/30.1.207 [PubMed: 11752295]
31. Chou TC. Theoretical basis, experimental design, and computerized simulation of synergism and antagonism in drug combination studies. (2006) Pharmacol Rev, 58:621–681. [PubMed: 16968952]
32. Crowe A, Zheng W, Miller J, Pahwa S, Alam K, Fung KM, et al. (2019). Characterization of Plasma Membrane Localization and Phosphorylation Status of Organic Anion Transporting Polypeptide (OATP) 1B1 c.521 T>C Nonsynonymous Single-Nucleotide Polymorphism. Pharm Res, 36(7), 101. doi:10.1007/s11095-019-2634-3 [PubMed: 31093828]
33. Crowe AR, & Yue W (2019). Semi-quantitative Determination of Protein Expression using Immunohistochemistry Staining and Analysis: An Integrated Protocol. Bio Protoc, 9(24). doi:10.21769/BioProtoc.3465
34. Wu J, & Houghton PJ (2010). Interval approach to assessing antitumor activity for tumor xenograft studies. Pharm Stat, 9(1), 46–54. doi:10.1002/pst.369 [PubMed: 19306260]
35. Merkle D, & Hoffmann R (2011). Roles of cAMP and cAMP-dependent protein kinase in the progression of prostate cancer: cross-talk with the androgen receptor. Cell Signal, 23(3), 507–515. doi:10.1016/j.cellsig.2010.08.017 [PubMed: 20813184]
36. Bhandari S, Peri A, Cranston I, McCool R, Shaw A, Glanville J,et al. (2017). A systematic review of known interventions for the treatment of chronic nonhypovolaemic hypotonic hyponatraemia

and a meta-analysis of the vaptans. Clin Endocrinol (Oxf), 86(6), 761–771. doi:10.1111/cen.13315 [PubMed: 28214374]

37. Morgenthaler NG, Struck J, Alonso C, & Bergmann A (2006). Assay for the measurement of copeptin, a stable peptide derived from the precursor of vasopressin. Clin Chem, 52(1), 112–119. doi:10.1373/clinchem.2005.060038 [PubMed: 16269513]
38. Rochais F, Vandecasteele G, Lefebvre F, Lugnier C, Lum H, Mazet JL, et al. (2004). Negative feedback exerted by cAMP-dependent protein kinase and cAMP phosphodiesterase on subsarcolemmal cAMP signals in intact cardiac myocytes: an in vivo study using adenovirus-mediated expression of CNG channels. J Biol Chem, 279(50), 52095–52105. doi:10.1074/jbc.M405697200 [PubMed: 15466415]
39. Sinha S, Dwivedi N, Tao S, Jamadar A, Kakade VR, Neil MO, et al. (2020). Targeting the vasopressin type-2 receptor for renal cell carcinoma therapy. Oncogene, 39(6), 1231–1245. doi:10.1038/s41388-019-1059-0 [PubMed: 31616061]
40. Marroncini G, Anceschi C, Naldi L, Fibbi B, Baldanzi F, Martinelli S, et al. (2021). Low sodium and tolvaptan have opposite effects in human small cell lung cancer cells. Mol Cell Endocrinol, 111419. doi:10.1016/j.mce.2021.111419
41. Garona J, Pifano M, Orlando UD, Pastrian MB, Iannucci NB, Ortega HH, et al. (2015). The novel desmopressin analogue [V4Q5]dDAVP inhibits angiogenesis, tumour growth and metastases in vasopressin type 2 receptor-expressing breast cancer models. Int J Oncol, 46(6), 2335–2345. doi:10.3892/ijo.2015.2952 [PubMed: 25846632]
42. Pastrian MB, Guzman F, Garona J, Pifano M, Ripoll GV, Cascone O, et al. (2014). Structure-activity relationship of 1-desamino-8-D-arginine vasopressin as an antiproliferative agent on human vasopressin V2 receptor-expressing cancer cells. Mol Med Rep, 9(6), 2568–2572. doi:10.3892/mmr.2014.2140 [PubMed: 24737067]
43. Ripoll GV, Garona J, Hermo GA, Gomez DE, & Alonso DF (2010). Effects of the synthetic vasopressin analog desmopressin in a mouse model of colon cancer. Anticancer Res, 30(12), 5049–5054. [PubMed: 21187489]
44. Sobol NT, Solerno LM, Beltran B, Vasquez L, Ripoll GV, Garona J, & Alonso DF (2021). Anticancer activity of repurposed hemostatic agent desmopressin on AVPR2-expressing human osteosarcoma. Exp Ther Med, 21(6), 566. doi:10.3892/etm.2021.9998 [PubMed: 33850538]
45. Khegay II, Popova NA, & Ivanova LN (2010). Reduced Walker 256 carcinosarcoma growth in vasopressin-deficient Brattleboro rats. Tumour Biol, 31(6), 569–573. doi:10.1007/s13277-010-0070-4 [PubMed: 20559788]
46. Cook LM, Shay G, Araujo A, & Lynch CC (2014). Integrating new discoveries into the “vicious cycle” paradigm of prostate to bone metastases. Cancer Metastasis Rev, 33(2-3), 511–525. doi:10.1007/s10555-014-9494-4 [PubMed: 24414228]
47. Tamma R, Sun L, Cuscito C, Lu P, Corcelli M, Li J,et al. (2013). Regulation of bone remodeling by vasopressin explains the bone loss in hyponatremia. Proc Natl Acad Sci U S A, 110(46), 18644–18649. doi:10.1073/pnas.1318257110 [PubMed: 24167258]
48. Fenner A (2019). AVPR1A: a target in CRPC? Nat Rev Urol, 16(9), 508. doi:10.1038/s41585-019-0218-y

Implications:

The arginine vasopressin signaling axis in castration resistant prostate cancer provides a therapeutic window that is targetable through repurposing safe and effective arginine vasopressin receptor type 1A and 2 antagonists.

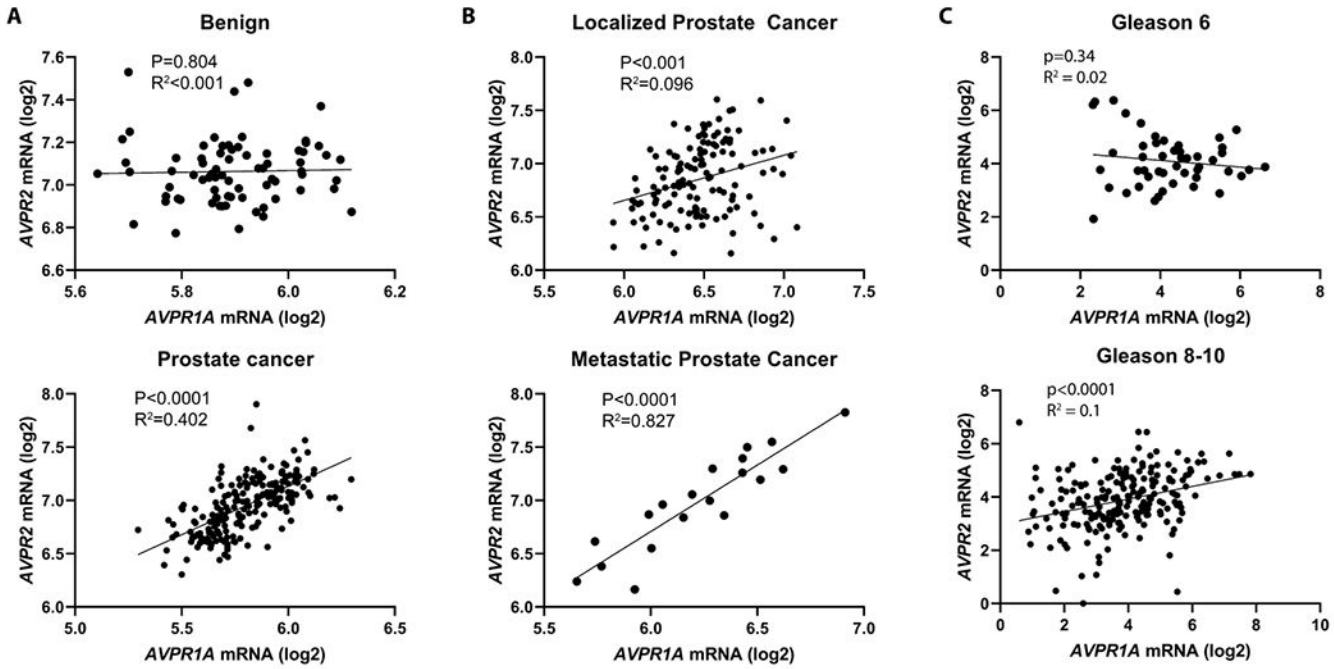

Figure 1. Expression of AVPR1A and AVPR2 mRNA is highly correlated in aggressive forms of prostate cancer.

(A) GSE70770 RNA-seq data base, (B) GSE21032 microarray data set, and (C) TCGA PRAD data set were analyzed for AVPR1A and AVPR2 co-expression. Values are expressed as log2-transformed signal intensity ratios, $p < 0.05$ was considered significant.

A

Cell Line	AVPR1A	AVPR2
RWPE-1	-	+
VCaP	+	-
LNCaP	-	+
C4-2B	+	+
22Rv1	+	+
PC3	-	-

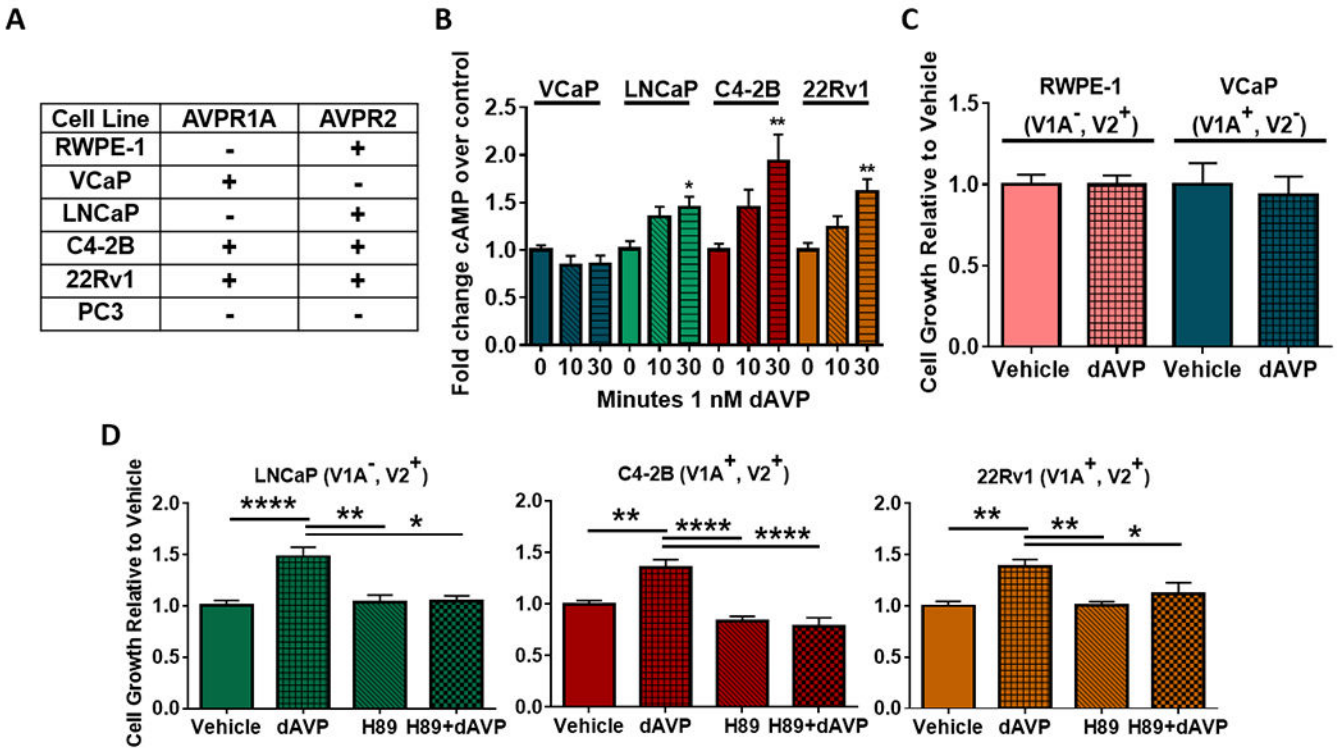

Figure 2. AVPR2 agonism promotes PKA-dependent castration resistant growth.

(A) Table of AVPR1A and AVPR2 mRNA status in the indicated prostate cell lines with "+" indicating detectable and "-" indicating non-detectable. (B) VCaP (N=2), LNCaP, C4-2B and 22Rv1 cells were treated with 1 nM dAVP (or vehicle) for the indicated timepoints. Intracellular cAMP was normalized to the vehicle. (C-D) Cells were androgen-depleted by incubation in serum-free media for 2 hours with one change of media and then cultured in 5% CSS containing media with vehicle, 1 μM dAVP (selective AVPR2 agonist), 1 μM H89 (PKA inhibitor) or dAVP plus H89 for 6 days with a media change at day 3. Live cells were counted. (RWPE-1 and VCaP N=2) "V1A" designates AVPR1A and "V2" designates AVPR2. *$p < 0.05$, **$p < 0.01$, **** $p < 0.0001$, error bars represent S.E.M.

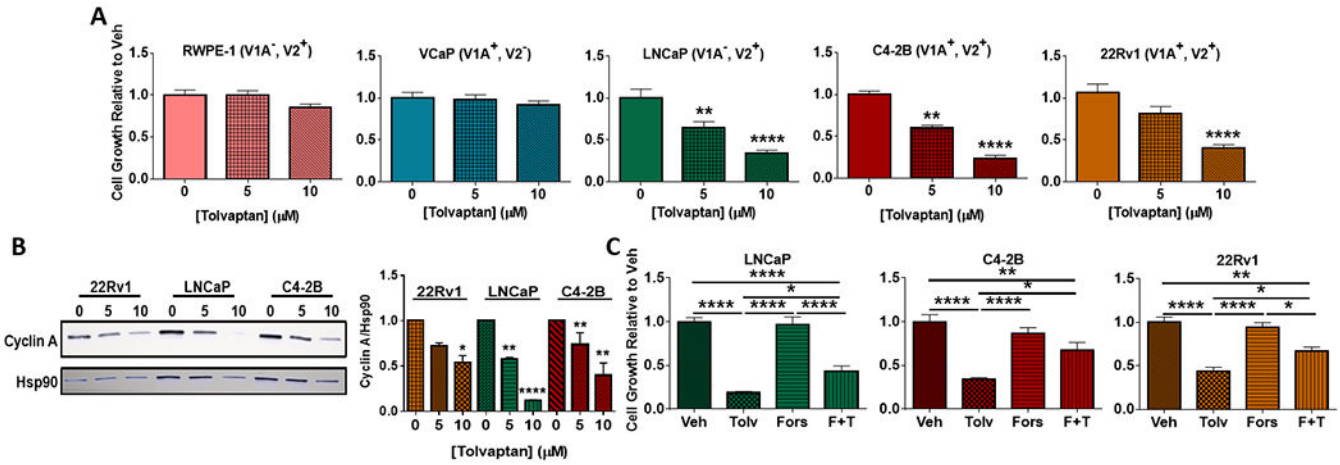

Figure 3. AVPR2 antagonism inhibits prostate cancer cell growth in a cAMP dependent manner.

(A) Cells were cultured for 6 days in media containing 2% FBS and the indicated concentrations of Tolvaptan (or vehicle) and live cells counted. (B) Cyclin A was analyzed by immunoblotting. [n=3 (C4-2B and LNCaP) or n=4 (22Rv1) independent experiments] Quantification of blots were performed using the KwikQuant Image Analyzer with the vehicle treated band set to 1 for each cell line. A one-sample t-test was used to determine if treatments were significantly different from 1. (C) Cells were treated with vehicle, 10 μM Tolvaptan, 500 nM forskolin or Tolvaptan plus forskolin for 6 days and live cells were counted. Veh = Vehicle, Tolv = Tolvaptan, Fors = Forskolin, F+T = Combination of Tolvaptan and Forskolin. *p < 0.05, **p < 0.01, ***p < 0.001, ****p < 0.0001, error bars represent S.E.M.

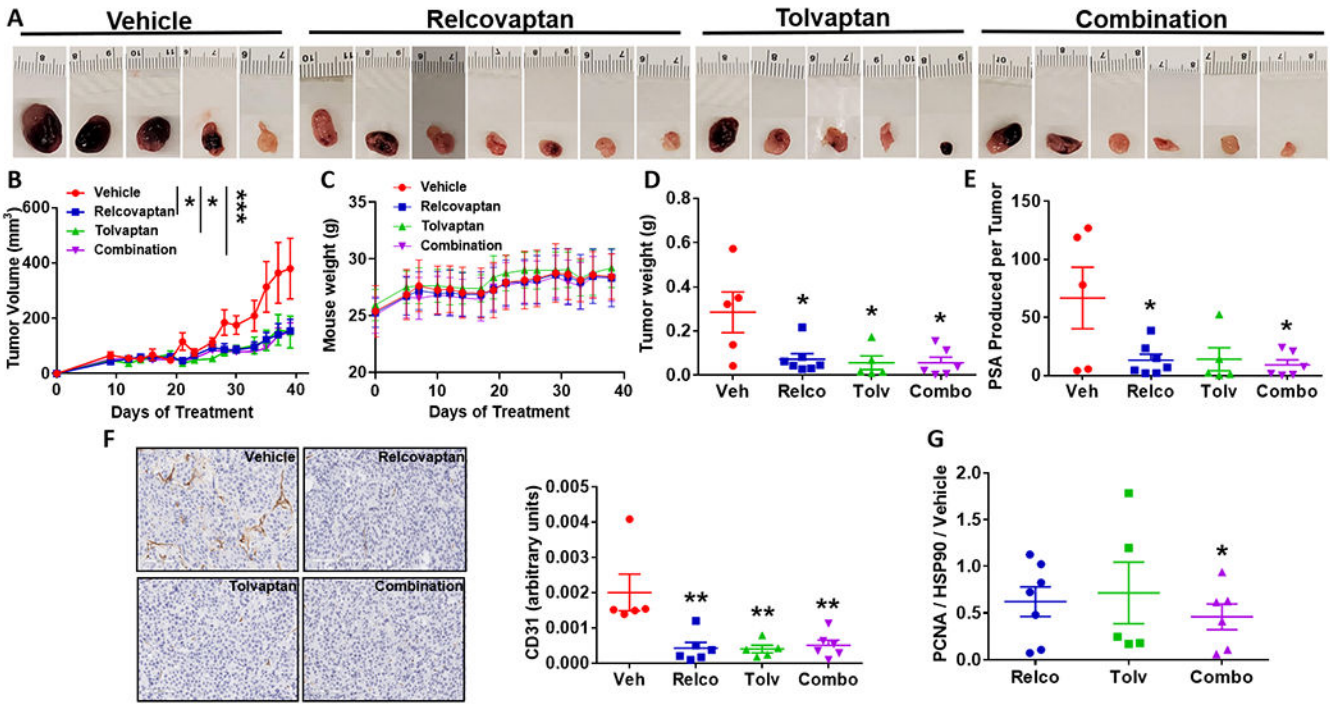

Figure 4. Dual inhibition of AVPR1A and AVPR2 reduces CRPC tumor growth in vivo.

Mice bearing C4-2B subcutaneous xenografts were treated daily (i.p.) with 50 mg/kg relcovaptan (n=7), 12.3 mg/kg tolvaptan (n=5), both (n=6) or vehicle (n=5). (A) Images of ex vivo tumors are shown. Scale represented by ruler in cm. (B) Significant differences in AUC for tumor volume are shown. (C) Mouse weights recorded during the study. (D) Ex vivo tumor weights are plotted. (E) PSA levels in sera are represented as the proportion of total tumor burden in each mouse. P=0.051 for tolvaptan treated mice. (F). Representative tumor images of CD31 immunostaining are shown (scale bar = 100 μm). Quantification of epitope staining is shown as arbitrary units of CD31 expression normalized to nuclei count. (G) Quantification of PCNA western blots. Data are shown as fraction of vehicle expression level. Relco = Relcovaptan, Combo = Combination of Relcovaptan and Tolvaptan. *p < 0.05, **p < 0.01, ***p < 0.001, error bars represent S.E.M.

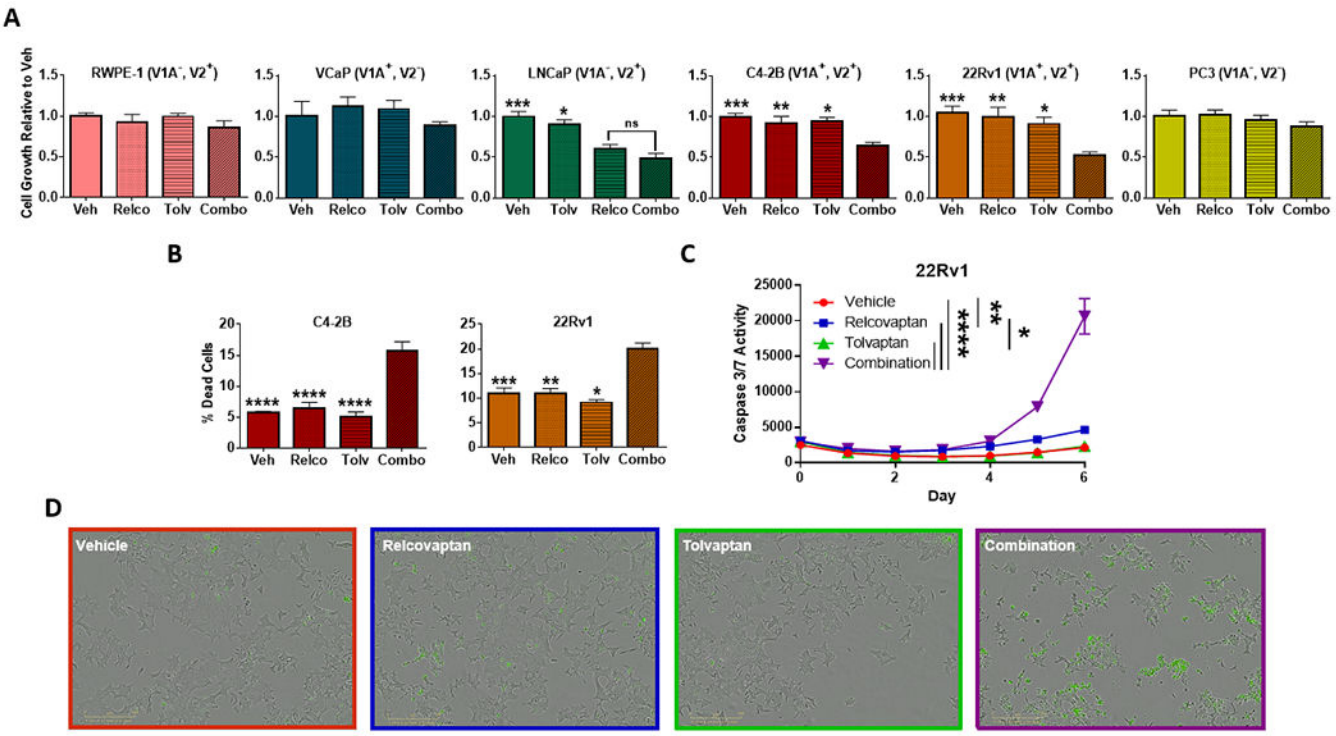

Figure 5. Relcovaptan and Tolvaptan synergistically inhibit CRPC growth and promote cell death.

(A) The indicated cell lines were treated with vehicle, 10 μM Relcovaptan (2.5 μM for C4-2B), 5 μM Tolvaptan (2.5 μM for C4-2B), or Relcovaptan plus Tolvaptan for 6 days. Live (A) and dead (B) cells were counted and compared to vehicle-treated cells set at 1. Significant differences between combination treatment and all other treatments is indicated. (C) 22Rv1 cells were incubated with the Incucyte Caspase 3/7 Reagent as well as vehicle, 10 μM Relcovaptan, 5 μM Tolvaptan, or Relcovaptan plus Tolvaptan and then imaged using the Incucyte Zoom. Total integrated green fluorescence (GCUx μm^2/image) was analyzed with the Incucyte Zoom software to determine caspase 3/7 activity, which was normalized to percent confluence. Data were analyzed via two-way ANOVA for significant differences between treatments at each time point. Significance shown is for day 6. (D) Representative images from Incucyte Zoom at day 6 are shown. *p<0.05, **p < 0.01, ***p < 0.001, ****p < .0001, ns = not significant, error bars represent S.E.M.

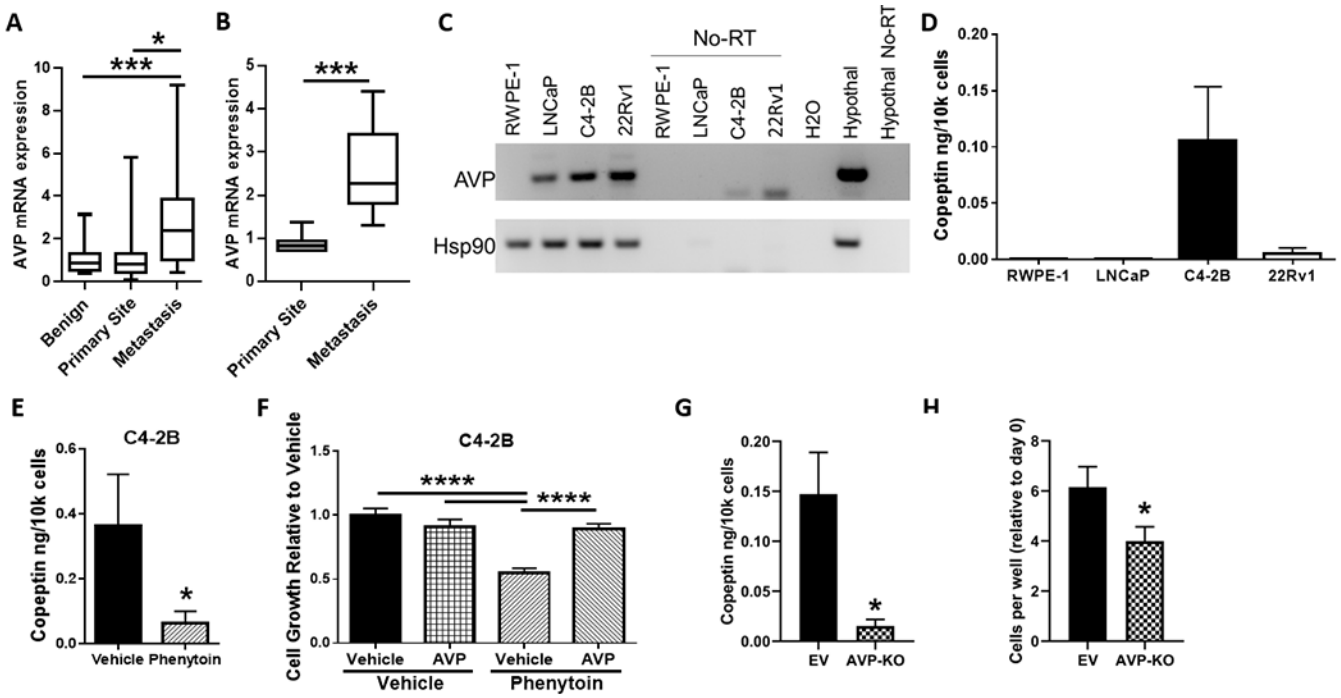

Figure 6. Advanced prostate cancer produces AVP.

Analysis of datasets (A) GSE35988 and (B) GSE6752 for AVP expression. Box plot bars are set to show min and max values. (C) RT-PCR was conducted on the indicated prostate cell lines. Human hypothalamic RNA served as a positive control. mRNA generated from samples with no reverse transcriptase (No-RT) added were included as negative controls. (D) Conditioned media from the indicated cell lines were analyzed by ELISA for copeptin. (E) Cells were treated with 100 μM phenytoin or vehicle for 48 hours and then copeptin was assessed in conditioned media. Copeptin production was normalized to amount per 10,000 cells. (F) Cells were treated with vehicle, 100 μM phenytoin, 100 nM AVP, or phenytoin plus AVP for 5 days then live cells were counted. (G) Conditioned media were analyzed by ELISA for copeptin. (H) Cells were cultured in media containing 5% CSS for 6 days and then counted. *p < 0.05, ***p < 0.001, ****p < .0001, error bars represent S.E.M.